Suitability of Blends from Virgin and Reprocessed Polylactide: Performance and Energy Valorization Kinetics

O. Gil-Castell[1], J. D. Badia[1,2] and A. Ribes-Greus[1,*]

[1] *Instituto de Tecnología de Materiales (ITM), Universitat Politècnica de València, Camino de Vera s/n, 46022 València, Spain*
[2]*Departament d'Enginyeria Química, Escola Tècnica Superior d'Enginyeria, Universitat de València, Av. de la Universitat s/n, 46100 Burjassot, Spain*

Received May 09, 2017; Accepted September 19, 2017

ABSTRACT: A blending strategy of virgin and reprocessed polylactide may be postulated as an alternative to reduce the material cost at industrial level, and as a valorization route to plastic waste management of production scraps. The performance of blends prepared from virgin polylactide and polylactide mechanically reprocessed up to two cycles (PLA-V/R) was assessed in terms of thermo-oxidative stability, morphology, viscoelasticity and thermal kinetics for energetic valorization. PLA-V/R blends showed appropriate thermo-oxidative stability. The amorphous nature of polylactide was preserved after blending. The viscoelastic properties showed an increment of the mechanical blend effectiveness, which suggested the feasibility of using PLA-V/R blends under similar mechanical conditions to those of virgin PLA goods. Finally, it was shown that the energetic valorization of PLA-V/R blends would result in a more feasible process, due to the lower required activation energy, thus highlighting the advantages of the energetic demand for the process. In conclusion, PLA-V/R blends showed similar processability, service performance and valorization routes as virgin PLA and therefore could be relevant in the sustainable circular industry of bioplastics.

KEYWORDS: Polylactide (PLA), mechanical recycling, reprocessing, energetic valorisation, thermal analysis

1 INTRODUCTION

The use of biobased materials, which have the benefit of coming from renewable resources and being biodegradable after their service life within a rational period of time, is a focus in the field of bioeconomy [1–5]. Polylactide (PLA) is a biodegradable, highly versatile aliphatic polyester produced by ring-opening polymerization of lactide, which can be obtained from renewable resources such as corn, beets, wheat and other starchy products [6, 7] and brings some interesting features consisting of appropriate mechanical and thermal properties, processability, recyclability and limited environmental impact [8, 9]. The great effort made in industrial production technology, has elevated PLA as a viable candidate for replacing commodities in several sectors [10–13].

Processing of PLA can be performed by means of several industrial techniques, such as injection molding or blow molding, or can be extruded into fibers, films and sheets. Accordingly, containers such as bottles or trays, and packaging films could feasibly be produced from PLA [5, 14]. An extended use of PLA in the packaging industry, among other goods, would result in the generation of a new considerable source of waste in the plastic fraction, among other commodities, which should therefore be managed. During service life, PLA can undergo thermal, photochemical and even biological degradation [15, 16]. Among the existing possibilities to deal with a high amount of bioplastic waste residues, mechanical recycling, energetic valorization and deposition in biodisposal facilities, such as composting plants, are the most established [17–20].

Mechanical recycling allows extending the service life of biobased polymeric materials before finally discarding them. It is a relatively simple procedure, requires low investment, and its technological parameters are currently controlled and can be considered in several stages of the life cycle of a given material. The recycling of industrial production off-cuts usually leads to a source of clean unused waste. This procedure usually consists of milling and shredding the production scraps and re-introducing them into the

**Corresponding author*: aribes@ter.upv.es

DOI: 10.7569/JRM.2017.634170

 DOI: 10.7569/JRM.2017.634170

processing facility to obtain the reprocessed material. Several attempts to reprocess PLA have been reported in the literature. Pillin *et al.* studied the influence of thermomechanical cycles of up to seven injection moldings [21], while Żenkiewicz *et al.* investigated the influence of multiple extrusion of PLA up to 10 times using a double-screw extruder for granulation of PLA followed by laboratory injection molding press [22]. Nascimento *et al.* evaluated the use of PLA industrial waste as a source of raw material for certain applications as well as the effects of annealing on the fracture behavior of PLA [23]. In addition, a detailed investigation of the behavior of PLA after multiple recycling steps using impact modifiers to improve mechanical properties was performed by Scaffaro *et al.* [24]. Badia *et al.* carried out a wide characterization of reprocessed PLA in terms of material valorization [25–27], hydrothermal ageing [28], dielectric properties [29] and energetic valorization [30, 31]. Beltrán *et al.* reported the influence of mechanical recycling on the hydrolytic performance of PLA [32]. All of these cited studies suggested that multiple reprocessing cycles greatly modified the stability of mechanical and thermal properties, as well as melt flow rate or permeability. The performance of recyclates reach a threshold and a non-suitable performance can be guaranteed for a given reprocessed material [33]. However, as studied by Badia and Ribes-Greus [27], the extent of degradation was noticeably influent from the second reprocessing step on, and allowed utilization of reprocessed PLA after 1 or 2 cycles for some existing applications.

Mechanical recycling can also be considered for the valorization of PLA waste after its service life, as long as external agents, such as oxygen, UV-light, mechanical stresses, temperature and water, promote degradation that might alter its long-term properties [34]. These degradation processes may modify the structure and composition of PLA and consequently change the thermal, viscoelastic and mechanical properties of the recyclates [18]. In addition, several stages are necessary in this case, such as collecting, washing, drying, shredding and reprocessing, which contribute to additional degradation [31]. This, along with the limited performance of recyclates upon multiple reprocessing cycles, suggested that some alternatives should be taken into account [34]. Some strategies consider the use of chain extenders [35], blending [36–38] or the preparation of composites [39]. When no more profit can be obtained from material valorization, energetic valorization is a viable solution to manage recycled plastic waste [20]. Thermally induced valorization technologies, such as pyrolysis, gasification and combustion, are commonly applied, and their feasibility shown for virgin and reprocessed PLA [30, 31].

In this work, the preparation of blends from reprocessed and virgin PLA was considered as a good alternative to not only reduce the material cost at industrial level, but also as a contribution to further plastic waste management solutions. In addition, a simulated thermally induced valorization procedure was taken into account to approach a hypothetical final service-life stage of energy valorization. In particular, the aim of the present study was to assess the performance of blends prepared from virgin and reprocessed polylactide in terms of thermal properties, morphology, viscoelasticity and thermal requirements for their energy valorization.

2 EXPERIMENTAL PROCEDURE

2.1 Material Description, Reprocessing Simulation and Sample Preparation

Polylactide (PLA) 2002D, a thermoforming grade PLA, was obtained from NatureWorks LLC as pellets, provided by AIMPLAS (Paterna, Spain). Prior to processing, virgin PLA (PLA-V) pellets were dried during 2 h at 80 °C in a Conair Micro-D FCO 1500/3 dehumidifier in order to remove the surface humidity. Afterwards, the samples were processed by means of injection molding with an Arburg 420 C 1000-350 single-screw injector. The temperature gradient set from hopper to nozzle was 160, 170, 190, 200 and 190 °C, whereas the molds were set at 15 °C. The cooling residence time was 40 s and the total residence time 60 s. The samples were dried before each processing cycle. After injection, the samples were ground by means of a Retsch SM 2000 cutting mill, which provided pellets of size d < 10 mm to be fed back into the process. Up to two processing cycles were applied under the same conditions to obtain the different testing specimens of reprocessed PLA (PLA-R1 and PLA-R2).

The blends of PLA-V and PLA-R were prepared by means of a twin-screw co-rotating extruder, with diameter D of 25 mm and L/D ratio of 24, from DUPRA S.L. The temperature gradient set from feed to die was 185, 185, 195 and 195 °C. After extrusion, the materials were ground by means of a Retsch SM 2000 cutting mill, which provided pellets of diameter < 10 mm.

Different compositions of PLA-V/R blends were prepared, from 40 to 80 wt% of reprocessed PLA, according to Table 1. Virgin and reprocessed PLA after 1 and 2 cycles are designated as V, R1 and R2, respectively.

Rectangular film-shaped samples were prepared by melt compression in a four axes compression press with a 120 × 10 × 0.2 mm^3 glass-fiber/Teflon® mold. The processing temperature was set at 170 °C. Five

Table 1 Blend compounding compositions. V stands for virgin PLA and R1/R2 for reprocessed PLA after 1 or 2 cycles, respectively.

Pure virgin PLA	Virgin/reprocessed PLA blends (composition in weight percentage)			Pure reprocessed PLA
PLA-V	V/R1			PLA-R1
	80/20	60/40	40/60	
	V/R2			PLA-R2
	80/20	60/40	40/60	

pressure steps were performed starting by preheating without pressure during 5 min, followed by 3 min at 50 kg·cm^{-2}, 3 min at 70 kg·cm^{-2} and 3 min at 100 kg·cm^{-2}, finalized by quenching at 15 °C during 2 h with released pressure. Finally, the samples were dried at 50 °C in a Heraeus Vacutherm VT 6025 vacuum oven during 24 h, kept in zip bags and placed in a desiccator at normalized lab conditions according to ISO 291 [40] for further analyses.

2.2 Analytic Techniques

2.2.1 Thermogravimetric Analysis (TGA)

The thermo-oxidative stability was analysed by means of a Mettler-Toledo TGA 851 thermogravimetric analyzer (TGA). The samples, with a mass of about 4 mg, were introduced in TGA Mettler-Toledo perforated alumina crucibles, with capacity of 70 µl. The samples were analyzed in the temperature range of 25 to 800 °C at different heating rates (β = 2, 5, 10, 15 and 20 °C·min^{-1}), under an oxygen atmosphere at a flow rate of 50 mL·min^{-1}. All experiments were performed in triplicate to ensure reproducibility of results.

2.2.2 Differential Scanning Calorimetry (DSC)

Calorimetric data were obtained by means of a Mettler-Toledo DSC 820 differential scanning calorimeter (DSC), calibrated following the procedure of In and Zn standards. The samples, with a mass of about 4 mg, were analyzed between 0 and 200 °C with a heating/cooling/heating profile at a rate of 10 °C·min^{-1}. All experiments were run under nitrogen atmosphere (50 mL·min^{-1}), performed in triplicate and the averages of enthalpies and temperatures were considered as representative values.

2.2.3 X-ray Diffraction (XRD)

X-ray diffraction analysis was performed by means of an X'Pert Pro diffractrometer model PW3040/60 to evaluate the crystallinity of PLA-V/R blends. Dried specimens of 100 mm^2 were considered for the analysis. The Cu Kα radiation (λ = 1.5418 Å) was generated with a tension of 45 kV and current of 35 mA and then monochromatized by using a Ni filter of 20 µm. The experiment was measured in the reflection mode at the angular range of 5–60° (2θ) and a scanning rate of 0.05° per 10 s. An average spectrum of three different specimens was considered as representative for each sample.

2.2.4 Dynamic-Mechanical-Thermal Analysis (DMTA)

Dynamic mechanical thermal analyses were conducted by the two-point bending mode in single cantilever clamping with 6 mm of effective length between clamps, by means of a Mettler-Toledo DMA 861e. The displacement was checked before all the experiments. The deformation force was set at 0.1 N and displacement amplitude at 10 µm. Experiments were carried out by heating from 35 °C to 130 °C with isothermal steps of 2 °C at 1 Hz of frequency. All experiments were performed in triplicate to ensure reproducibility.

3 RESULTS AND DISCUSSION

The performance of the PLA-V/R blends was initially assessed in terms of thermo-oxidative stability by thermogravimetry. Afterwards, the morphology of PLA-V/R blends, along with their thermal properties, were evaluated by differential scanning calorimetry and X-ray diffraction. In addition, the viscoelastic behavior and the mechanical blending effectiveness were characterized by dynamic thermal mechanical analysis. Finally, the energetic valorization of future PLA-V/R wastes was simulated by kinetic studies of their thermo-oxidative decomposition behavior.

3.1 Material Valorization: Blends of Virgin and Reprocessed Polylactide

3.1.1 Thermo-oxidative Stability of PLA-V/R Blends

The analysis of the thermo-oxidative stability was focused on the study of the safety limit temperatures of PLA-V/R blends. In this section, a study of the decomposition profiles of PLA-V/R blends subjected to an oxidizing atmosphere was performed by means of thermogravimetric analysis (TGA). In addition, multi-rate linear non-isothermal experiments were carried out in order to functionalize the evolution of

 DOI: 10.7569/JRM.2017.634170

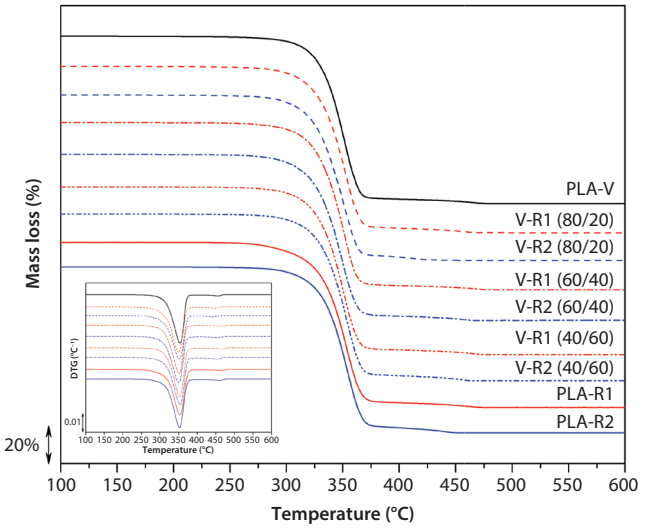

Figure 1 Decomposition profiles of the thermogravimetric curve (TG) and first-derivative thermogravimetric curve (DTG, inset) for virgin (PLA-V), reprocessed (PLA-R1 and PLA-R2) and virgin/reprocessed PLA blends (V/R).

the thermo-oxidative stability at any linear heating rate (β), set the TDB function and the zero-decomposition temperatures [41], as explained hereby.

Figure 1 shows the decomposition profiles (TG) and the first-derivative curves (DTG) for all PLA-V/R blends at 10 °C·min^{-1}. The rest of the TGA experiments with different heating rates showed similar profiles and are not shown for the sake of clarity. The thermograms showed a general mass loss of ~97–98%, regardless of the composition of the PLA-V/R blend. They exhibited three differentiated mass-loss stages, in accordance with reported results for PLA-based materials [17, 31, 42]. The first slight initial loss up to 100 °C—omitted in the plot—can be related to remnant water present in the materials. Then, the decomposition of the PLA backbone took place, from ~275 to ~375 °C, with a peak around ~352 °C for all compounded materials. Finally, from ~375 °C to ~500 °C, the degradation of char formed during previous decomposition was observed, with a peak around ~450 °C.

The decomposition profiles were characterized in terms of the decomposition onset (T_o) and endset (T_e) temperatures from the TG curve and the peak temperature (T_p) from the DTG curves. The values of these parameters along with the mass-loss percentage at 600 °C ($\Delta m_{600\,°C}$) are gathered in Table 2. Virgin and reprocessed PLA showed almost identical values. Blending often produced a minor decrease in the thermo-oxidative stability, more perceptible in the onset temperature (T_o). However, the differences are almost irrelevant, regardless of the blend composition.

Table 2 Thermogravimetric data at β = 10 °C · min^{-1} in terms of onset temperature (T_o), peak temperature (T_p), endset temperature (T_e) and final mass loss (Δm) for virgin (PLA-V), rep·rocessed (PLA-R1 and PLA-R2) and virgin/reprocessed PLA blends (V/R).

	T_o (°C)	T_p (°C)	T_e (°C)	$\Delta m_{600\,°C}$ (%)
PLA-V	329.6 ± 1.2	351.9 ± 1.1	365.0 ± 0.3	98.9 ± 0.1
V-R1 (80/20)	326.6 ± 1.4	350.7 ± 1.3	364.2 ± 0.9	98.1 ± 0.1
V-R1 (60/40)	327.6 ± 0.4	351.2 ± 0.3	363.7 ± 0.7	98.1 ± 0.1
V-R1 (40/60)	327.8 ± 1.7	351.8 ± 0.8	365.2 ± 0.6	97.2 ± 0.1
PLA-R1	329.4 ± 0.7	352.8 ± 0.7	366.2 ± 0.5	97.2 ± 0.3
V-R2 (80/20)	325.1 ± 0.7	350.6 ± 1.0	364.6 ± 0.8	97.6 ± 0.1
V-R2 (60/40)	325.9 ± 0.3	349.7 ± 0.3	363.2 ± 0.1	98.0 ± 0.3
V-R2 (40/60)	329.9 ± 0.6	353.6 ± 0.4	366.4 ± 0.4	98.0 ± 0.2
PLA-R2	330.5 ± 0.5	353.0 ± 0.6	366.8 ± 1.1	97.4 ± 0.1

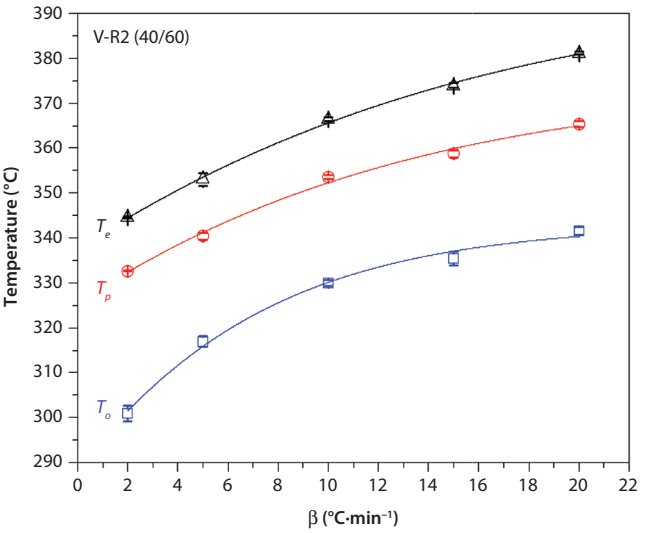

Figure 2 Application of the TDB model to fit the evolution of T_o, T_p and T_e for the virgin/reprocessed—V-R2 (40/60)—blend.

The aim was to enhance the analysis of the influence of the heating rate β on the characteristic decomposition temperatures studied above (T_o, T_p and T_e). At high β the evolution of the parameters is almost linear, whereas at low β a curved tendency was observed. The so-called thermal decomposition behavior (TDB) model given in Equation 1 was proposed [31]. An example of its validity is shown in Figure 2 for the case of the blend V-R2 (40/60).

$$TDB(\beta) = \frac{a}{1 + b \cdot e^{-k \cdot \beta}} \quad (1)$$

Table 3 Results of fitting T_o = f (β) to Equation 2, along with the onset zero-decomposition temperature obtained by extrapolating Equation 2 to $\beta \to 0$ for virgin (PLA-V), reprocessed (PLA-R1 and PLA-R2) and virgin/reprocessed PLA blends (V/R).

TDB fitting values for T_o								
	a		b		k		R^2	*ZDT* (ºC)
	a	e (%)	b	e (%)	k	e (%)		
PLA-V	340.7	0.58	0.17	2.40	0.17	3.24	0.99	290.2
V-R1 (80/20)	345.8	0.19	0.20	2.50	0.13	3.49	0.99	287.1
V-R1 (60/40)	344.7	0.54	0.22	4.20	0.16	5.26	0.98	283.5
V-R1 (40/60)	346.2	0.36	0.21	4.36	0.14	5.92	0.97	286.6
PLA-R1	344.6	0.31	0.19	4.93	0.16	5.68	0.98	289.8
V-R2 (80/20)	341.6	0.34	0.21	4.82	0.15	5.93	0.98	283.1
V-R2 (60/40)	342.4	0.40	0.23	5.71	0.18	4.67	0.98	279.2
V-R2 (40/60)	343.1	0.16	0.19	5.79	0.16	3.38	0.99	288.6
PLA-R2	344.9	0.27	0.19	4.31	0.16	5.85	0.99	290.3

The so-called zero-decomposition temperature (*ZDT*) was considered to evaluate the differences in the thermal stability under oxidative conditions, instead of choosing the experimental temperatures obtained at a specific β, since this parameter is related to the induction of the decomposition. *ZDT* can be obtained by extrapolating the TDB function of T_o to infinitely low β [30]. Table 3 gathers the results of the TDB fitting and the ZDT_o. Almost identical values of ZDT_o were found for virgin and reprocessed PLA. However, all blends exhibited lower ZDT_o values, especially those of 60% of virgin and 40% of both reprocessed PLA, with a reduction between 3 and 8 °C, representing a maximum of ~2.8% decrease with respect to PLA-V. Blending often produced a minor decrease in the thermo-oxidative stability, through the reduction in the ZDT_o. The presumable presence of more sites available to the penetration of the O_2 in the blended structures may have promoted decomposition at slightly lower temperatures. The slight reduction of the thermo-oxidative stability is assumable and therefore the PLA-V/R blends present a safe temperature margin, similar to that shown by virgin and reprocessed PLA.

3.1.2 Calorimetric Thermal Properties and Morphology of PLA-V/R Blends

The aim of the calorimetric analysis was to evaluate the influence of the addition of reprocessed PLA into virgin PLA on the amorphous/crystalline morphological balance [42–47]. A first heating scan was carried out to remove thermal history and ascertain the effect of the processing through melt compression. Then, cooling and second heating scans were considered to intrinsically study the prepared materials. The PLA matrix structural relaxation, cold crystallization and melting were evaluated from heating scans. The temperature (T_{sr}) and enthalpy (Δh_{sr}) associated with the structural relaxation were evaluated from its peak and area using constant integration limits and a smooth polynomial function (sp-line) as baseline. The cold-crystallization and melting temperatures (T_{cc} and T_m) were determined from their peaks in thermograms and the enthalpies associated with those events (Δh_{cc} and Δh_m) were determined using constant integration limits. The degree of crystallinity (X_c) was calculated by means of Equation 2:

$$X_c = \frac{(\Delta h_m - |\Sigma \Delta h_{cc}|)}{\Delta h_{m0}} \times 100 \qquad (2)$$

where Δh_{m0} is the melting enthalpy for a 100% crystalline PLA (93 J·g^{-1} [48]). The glass transition temperature (T_g) was obtained from the cooling scan through a tangential method. The results of the main temperatures and enthalpies are gathered in Tables 4, 5 and 6 for the first heating, cooling and second heating scans, respectively.

The effect of the blend processing into films through melt compression was evaluated from the data gathered in Table 4. The cold-crystallization and melting enthalpies were almost equal for all virgin, reprocessed and PLA-V/R blends, which suggested that all materials remained amorphous, without relevant formation of a crystalline phase. This fact was confirmed by X-ray diffraction, as shown in Figure 3. The crystallinity of PLA is related to sharp reflection peaks positioned at 16.8°, 19.1° and 22.6°, corresponding to the (200)/(110), (203), (210) planes respectively [49]. Although some smooth peaks can be intuited at characteristic positions of semicrystalline PLA, the spectra obtained for all materials showed a wide diffraction band from

Table 4 Calorimetric data of the first heating scan for virgin (PLA-V), reprocessed (PLA-R1 and PLA-R2) and virgin/reprocessed PLA blends (V/R).

1st heating	Δh_{sr} (J · g^{-1})	T_{sr} (°C)	Δh_{cc} (J · g^{-1})	T_{cc} (°C)	Δh_m (J · g^{-1})	T_m (ºC)
PLA-V	2.3 ± 0.1	58.5 ± 0.2	–4.5 ± 1.9	118.2 ± 0.4	4.1 ± 2.6	149.8 ± 0.2
V-R1 (80/20)	0.9 ± 0.1	58.6 ± 0.2	–12.6 ± 0.7	128.6 ± 0.4	12.7 ± 0.8	152.5 ± 0.4
V-R1 (60/40)	1.1 ± 0.1	58.7 ± 0.2	–11.1 ± 0.2	128.7 ± 0.1	11.4 ± 0.3	151.8 ± 0.4
V-R1 (40/60)	1.3 ± 0.1	58.9 ± 0.1	–9.4 ± 1.1	127.3 ± 0.5	9.9 ± 0.7	150.8 ± 0.2
PLA-R1	1.6 ± 0.1	60.3 ± 0.1	–2.2 ± 0.6	120.1 ± 0.1	1.4 ± 0.1	148.5 ± 0.5
V-R2 (80/20)	1.4 ± 0.1	58.4 ± 0.1	–16.4 ± 0.7	127.1 ± 0.2	16.4 ± 0.2	150.7 ± 0.2
V-R2 (60/40)	1.6 ± 0.1	59.3 ± 0.7	–12.1 ± 0.1	128.4 ± 0.2	12.4 ± 0.4	152.1 ± 1.1
V-R2 (40/60)	1.5 ± 0.1	59.5 ± 0.6	–7.2 ± 0.1	128.7 ± 0.7	8.0 ± 0.4	151.4 ± 0.5
PLA-R2	0.4 ± 0.1	57.9 ± 0.1	–1.3 ± 0.3	122.9 ± 1.3	1.5 ± 0.1	149.3 ± 0.1

Table 5 Glass transition temperatures (T_g) of virgin (PLA-V), reprocessed (PLA-R1 and PLA-R2) and virgin/reprocessed PLA blends (V/R).

Cooling	T_g (ºC)
PLA-V	54.9 ± 0.2
V-R1 (80/20)	55.4 ± 0.1
V-R1 (60/40)	55.9 ± 0.1
V-R1 (40/60)	55.6 ± 0.1
PLA-R1	55.9 ± 0.1
V-R2 (80/20)	55.6 ± 0.1
V-R2 (60/40)	55.6 ± 0.2
V-R2 (40/60)	55.9 ± 0.2
PLA-R2	55.7 ± 0.1

10 to 25°, which is characteristic of the scattering of amorphous PLA [50–52]. Therefore, film processing through melt compression, followed by a quenching procedure, seems to have inhibited the development of crystallinity, resulting in an unordered amorphous structure.

During the cooling scan, a single glass transition was found. The absence of any crystallization phenomenon corroborated the amorphous character of the materials. The glass transition temperature (T_g), remained at 55 ± 1 °C for virgin, reprocessed PLA and all PLA-V/R blends, as gathered in Table 5. Reprocessing and subsequent blending did not significantly influence the glass transition of the material. Therefore, the thermal service conditions of PLA-V/R blends remained unaltered, in comparison to those of virgin PLA.

The second heating scan showed the intrinsically thermal properties of the different materials, whose calorimetric spectra are compared in Figure 4. In all cases, the structural relaxation associated with the physical aging occurred at similar peak temperatures and enthalpies, as gathered in Table 6. Afterwards, a cold crystallization was observed, almost imperceptible for virgin and reprocessed PLA separately, though highly pronounced for blends. Next, a melting event was found, smooth for virgin and reprocessed PLA but more intense for blended materials. The enthalpies associated with the cold crystallization and melting were higher for virgin-rich PLA blends and diminished when the content of reprocessed PLA increased. Nevertheless, the PLA-V/R blends preserved the amorphous morphology, which suggested usability of goods of PLA-V/R similar to that of virgin PLA.

3.1.3 Viscoelastic Performance of PLA-V/R Blends

The evolution of the storage modulus (E') and loss modulus (E'') recorded as a function of temperature is plotted in Figure 5 to evaluate the effects of blending on the viscoelastic performance of PLA [53]. The maximum of the loss modulus is associated with the cooperative movements greatly influenced by the viscous contribution of the main chain of macromolecules constituting the amorphous region. These movements are considered precursors of the glass transition [54]. When the reprocessed and virgin materials were blended, the temperature calculated for the loss modulus peak barely changed, which would confirm that the amorphous region undergoes non-significant modifications.

The storage modulus (E') in the linear scale showed an initial rigidity plateau followed by a drastic drop that started at ~45 °C, associated with the glass-rubber relaxation of the polymer chains, which takes place around the glass transition temperature, characteristic for PLA-based materials [55]. After the glass-rubber relaxation, a small increase in the E' modulus was found, which is related to the cold-crystallization phenomenon, as

Table 6 Calorimetric data of the second heating scan for virgin (PLA-V), reprocessed (PLA-R1 and PLA-R2) and virgin/reprocessed PLA blends (V/R).

2nd heating	Δh_{sr} (J·g^{-1})	T_{sr} (ºC)	Δh_{cc} (J·g^{-1})	T_{cc} (ºC)	Δh_{m} (J·g^{-1})	T_{m} (ºC)
PLA-V	1.0 ± 0.1	61.3 ± 0.1	–3.5 ± 1.8	129.2 ± 0.7	3.7 ± 1.6	152.0 ± 0.1
V-R1 (80/20)	1.0 ± 0.1	61.3 ± 0.1	–12.3 ± 0.7	129.5 ± 0.1	12.4 ± 0.7	152.5 ± 0.1
V-R1 (60/40)	0.9 ± 0.1	61.7 ± 0.1	–8.4 ± 0.1	129.8 ± 0.1	8.8 ± 0.3	152.0 ± 0.2
V-R1 (40/60)	0.7 ± 0.1	61.8 ± 0.1	–8.0 ± 0.1	129.1 ± 0.2	8.2 ± 0.1	151.3 ± 0.1
PLA-R1	1.3 ± 0.1	62.1 ± 0.1	–0.2 ± 0.2	129.9 ± 0.1	0.2 ± 0.1	149.7 ± 0.2
V-R2 (80/20)	1.4 ± 0.1	61.4 ± 0.1	–13.7 ± 0.5	128.3 ± 0.1	13.9 ± 0.6	151.2 ± 0.1
V-R2 (60/40)	0.9 ± 0.1	61.6 ± 0.1	–11.4 ± 0.1	129.2 ± 0.1	12.1 ± 0.3	151.6 ± 0.1
V-R2 (40/60)	1.1 ± 0.1	61.9 ± 0.1	–6.4 ± 0.2	129.8 ± 0.2	6.6 ± 0.3	151.3 ± 0.1
PLA-R2	1.4 ± 0.3	62.3 ± 0.1	–0.6 ± 0.1	129.2 ± 2.1	0.6 ± 0.1	150.2 ± 0.1

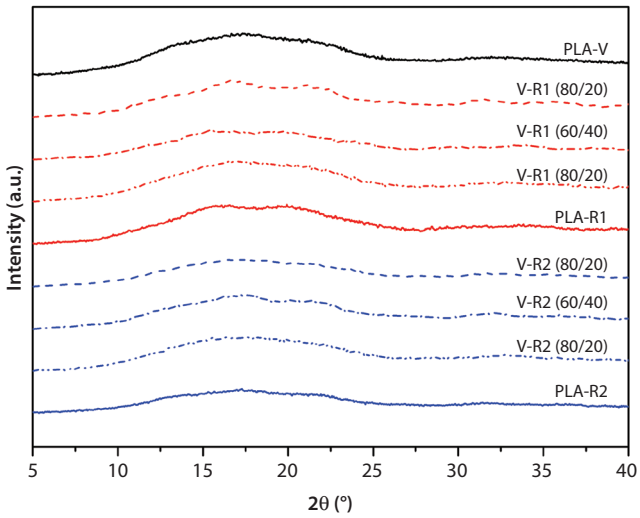

Figure 3 X-ray diffraction patterns for virgin (PLA-V), reprocessed (PLA-R1 and PLA-R2) and virgin/reprocessed PLA blends (V/R).

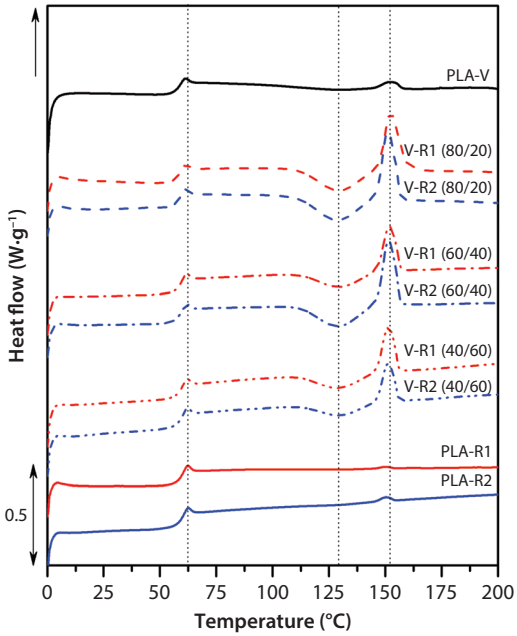

Figure 4 DSC curves of the second heating scan for virgin (PLA-V), reprocessed (PLA-R1 and PLA-R2) and virgin/reprocessed PLA blends (V/R).

observed by calorimetric analysis in the previous section. That new crystalline structure brought some rigidity to the entire material, which implied a higher E'. The cold-crystallization event followed a different pattern for virgin PLA, reprocessed PLA and blends. PLA-V/R blends generally concluded the cold crystallization at lower temperatures, which suggested that blending virgin and reprocessed PLA favored crystallization during heating, as advised by differential scanning calorimetry. This fact, however, does not affect the usual applications of PLA goods in the glassy state.

The study of the storage modulus at 35 °C can provide a general overview of the rigidity of PLA-V/R blends in the glassy state, as plotted in Figure 6. Both reprocessed PLAs showed slightly higher elastic modulus than the virgin PLA, according to previous studies [21, 23]. Higher rigidity was found for all PLA-V/R blends regardless the composition, reaching similar values between ~2800 and ~3000 MPa, representing a ~33% increase with respect to virgin PLA. The presence of dissimilar size polymeric chains may have enhanced the occurrence of more entanglements, which provoked higher rigidity.

The mechanical blending effectiveness (*MBE*), considered as an indicator of the rigidizing or reinforcement degree in the preparation of polymer blends and composites [56–58], was calculated according to Equation 3, where E'_g and E'_r are the storage modulus values in the glassy and rubbery region, respectively.

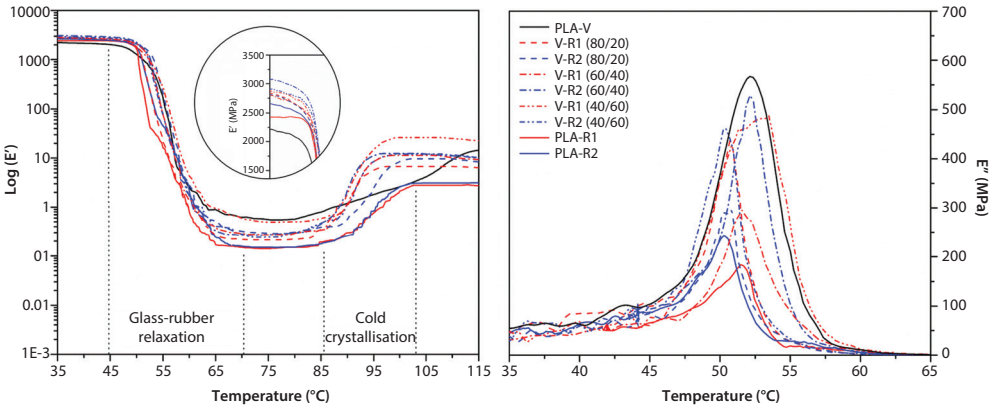

Figure 5 Evolution of storage modulus (E') as a function of temperature at a frequency of 1 Hz for virgin (PLA-V), reprocessed (PLA-R1 and PLA-R2) and virgin/reprocessed PLA blends (V/R).

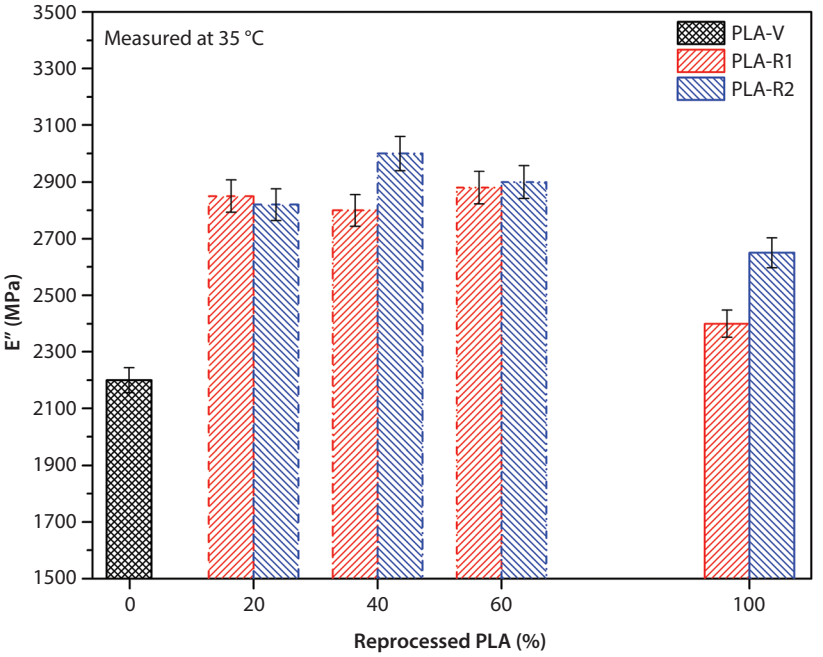

Figure 6 Storage modulus (E') evolution as a function blend composition measured at 35 °C and a frequency of 1 Hz.

The higher the value of the parameter *MBE*, the higher is the effectiveness of the blending.

$$MBE = 1 - \frac{(E_g' / E_r')_{blend}}{(E_g' / E_r')_{PLA-V}} \quad (3)$$

Figure 7 shows the values of the *MBE*, taking the measured E' values at 35 °C and 100 °C at 1 Hz as E'_g and E'_r respectively. Due to reprocessing, lower *MBE* was found for both reprocessed PLA-R1 and PLA-R2, in comparison to that of virgin PLA-V. However, a general increase of *MBE* was encountered after blending, which was similar regardless of the type of reprocessed PLA incorporated into the blend. The increase of *MBE* was higher when there was more reprocessed PLA content in the blend.

3.1.4 Energetic Valorization: Thermal Kinetics of the Thermo-oxidative Decomposition of Blends of Virgin and Reprocessed Polylactide

The thermal kinetics of the thermo-oxidative decomposition behavior were assessed in terms of activation energy in order to simulate further energetic valorization of PLA-based wastes [34]. The methodology followed in this analysis is reported elsewhere [41]. Briefly, the apparent activation energy

of the thermo-oxidative decomposition process was evaluated as a function of the conversion degree. The applied isoconversional methods were based on linear integral approaches, expressly those developed by Flynn-Wall-Ozawa (FWO) [59, 60] and Kissinger-Akahira-Sunose (KAS) [61, 62], both gathered in Table 7, where α is the conversion degree, β is the TGA heating rate, A is the Arrhenius pre-exponential factor, $g(\alpha)$ is the kinetic function, T is the temperature and Ea is the apparent activation energy. For a given degree of conversion (α) and heating rate (β), a characteristic temperature T_α was calculated for each material. The degree of conversion was considered from 0.05 to 0.95 in 0.05 increasing gaps, and heating rates considered were 2, 5, 10, 15 and 20 °C·min^{-1}. Figure 8 shows the results of the thermogravimetric analysis.

The representation of the FWO and KAS plots for a given material, in this case the blend V-R2 (40/60), is shown in Figure 8a,b as a model to ascertain the linearity of the plots. The rest of materials, which are omitted for the sake of conciseness, showed similar plots. From the slope of these representations, the apparent activation energy was calculated, and its evolution given as a function of the degree of conversion (Ea_α). As can be seen in Figure 8c, both methods offered similar Ea_α values, showing a good coincidence along the decomposition process, as obtained for the rest of PLA-V/R blends. It was found that experimental Ea_α data could be adjusted to Equation 4 in order to define a model to calculate activation energy for any conversion degree [41],

$$Ea(\alpha) = Ea^I + \left(Ea^{II} - Ea^I\right)\cdot e^{-\frac{\alpha}{p}} \quad (4)$$

where Ea^I and Ea^{II} are parameters that can be obtained from the intercept at $\alpha = 0$ and in the asymptote, giving an idea of the amplitude of decomposition, and p is a power to correct the function curvature, ranging from 0 to 1. A low p value (close to 0) indicated an Ea becoming almost constant, while higher p (close to 1) approached linear tendencies. Results for this parameters as well as the regression coefficient that verifies the suitability of this equation are gathered in Table 8.

The averaged values of the apparent activation energy obtained by the FWO and KAS methods, with a standard deviation lower than 5%, were plotted for all cases in Figure 8d. A significant variation in apparent activation energy along the decomposition process was observed following an exponential growing fashion for PLA-V, PLA-R1/R2 and PLA-V/R blends, in agreement with previous analysis [30]. The Ea_α increased from ~80–110 kJ·mol^{-1} at low conversions to ~150–200 kJ·mol^{-1} at the end of decomposition. Blending provoked similar Ea_α values to reprocessed PLA at low conversion degrees whereas showed lower activation energy at high conversion degrees. In general, PLA-V/R blends showed Ea_α values lower than those given by virgin PLA-V and both reprocessed PLA-R1/R2, in a ~15 kJ·mol^{-1} range, which was narrower than that given by PLA-V and PLA-R1/R2. Therefore, from a cost-effective point of view, considering the energetic demand of each material, the combustion of PLA-V/R blends would result in an advantageous energetic process, thus highlighting the feasibility of the energetic demand for the valorization of their wastes.

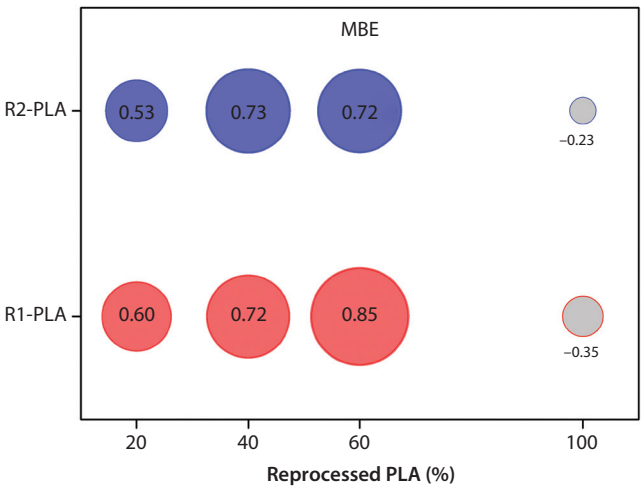

Figure 7 Mechanical blending effectiveness values (*MBE*), considering the measured E' at 35 °C and 100 °C at 1 Hz as E'_g and E'_r respectively, as a function of the reprocessed PLA content (PLA-R1/R2).

Table 7 Isoconversional methods used to calculate the apparent activation energy.

Method designation	Equation
Flynn-Wall-Ozawa (FWO) [59, 60] (supported on Doyle's integral approximation [63])	$\left[\log(\beta)\right]_y = \log\left(\frac{A_\alpha \cdot Ea_\alpha}{R \cdot g(\alpha)}\right) - 2.315 - \frac{0.457 \cdot Ea_\alpha}{R} \cdot \left[\frac{1}{T_\alpha}\right]_x$
Kissinger-Akahira-Sunose (KAS) [61, 62]	$\left[\ln\left(\frac{\beta}{T_\alpha^2}\right)\right]_y = \ln\left(\frac{A_\alpha \cdot R}{Ea_\alpha \cdot g(\alpha)}\right) - \frac{Ea_\alpha}{R} \cdot \left[\frac{1}{T_\alpha}\right]_x$

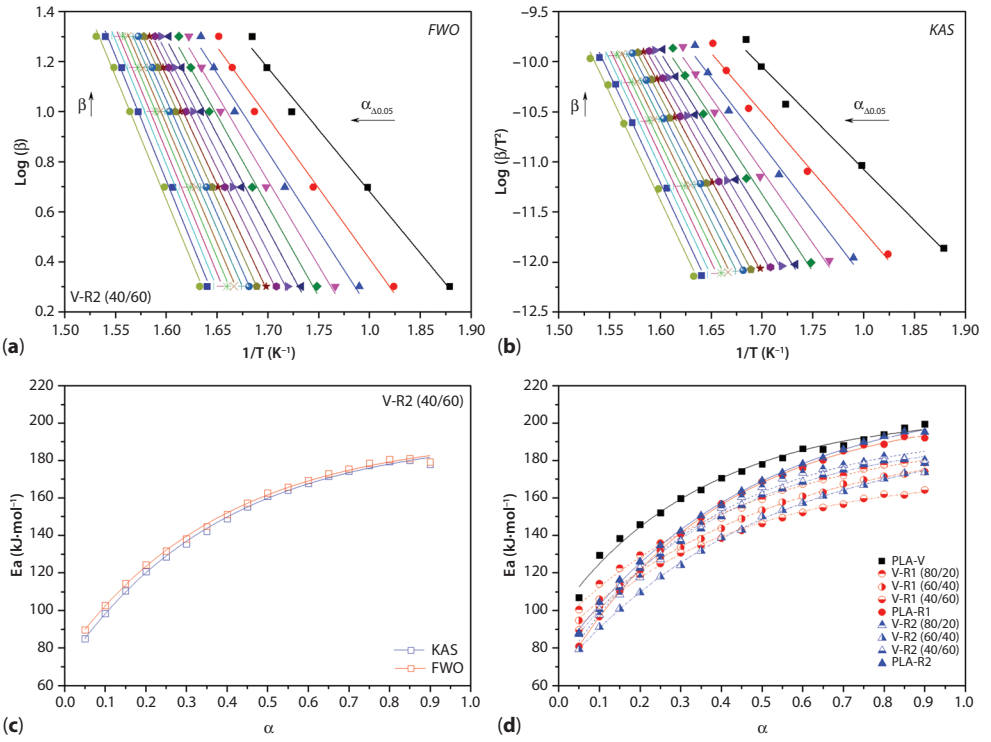

Figure 8 (**a**) Flyn-Wall-Ozawa (*FWO*) and (**b**) Kissinger-Akahira-Sunose (*KAS*) thermo-oxidative degradation representations for the compounded blend V-R2 (40/60); (**c**) calculated activation energy as a function of conversion degree through *FWO* and *KAS* for the compounded blend V-R2 (40/60); (**d**) averaged calculated activation energies (symbols) and theoretical model (lines), as a function of conversion degree for virgin (PLA-V), reprocessed (PLA-R1 and PLA-R2) and virgin/reprocessed PLA blends (V/R). Error bars were omitted for the sake of clarity.

Table 8 Fitting parameters of the theoretical model to calculate activation energy for any conversion degree for virgin (PLA-V), reprocessed (PLA-R1 and PLA-R2) and virgin/reprocessed PLA blends (V/R).

	Ea^{I}		Ea^{II}		p		R^2
	value (kJ)	e (%)	value (kJ)	e (%)	value	e (%)	
PLA-V	206	1.52	99	1.38	0.36	1.80	0.990
V-R1 (80/20)	208	0.75	64	1.90	0.39	0.56	0.999
V-R1 (60/40)	218	1.21	76	1.84	0.48	0.67	0.998
V-R1 (40/60)	196	1.71	93	1.85	0.48	1.15	0.995
PLA-R1	194	1.26	86	1.27	0.52	0.70	0.998
V-R2 (80/20)	173	1.04	81	1.70	0.40	1.00	0.997
V-R2 (60/40)	197	1.72	68	1.99	0.38	1.48	0.993
V-R2 (40/60)	196	1.08	68	1.47	0.50	0.53	0.999
PLA-R2	195	1.06	73	2.20	0.40	0.88	0.997

4 CONCLUSIONS

Blends of virgin and reprocessed polylactide (PLA-V/R) were obtained by the usual industrial machinery, under typical processing parameters for virgin PLA. The performance of PLA-V/R blends was assessed in terms of thermo-oxidative stability, morphology, viscoelasticity and energetic requirements for decomposition kinetics.

The slight reduction of the zero-decomposition temperature ZDT_0 of the PLA-V/R blends was technically assumable and presented a safe temperature

margin similar to that of virgin and reprocessed PLA. Therefore, PLA-V/R blends showed appropriate thermo-oxidative stability.

The PLA-V/R blends kept the amorphous nature of polylactide, regardless of the type and/or amount of reprocessed PLA in the formulation of the blend. The PLA-V/R blends did not modify the glass transition of the material so it could be used in applications with similar thermal service conditions to those of virgin PLA-V.

The storage modulus of PLA-V/R blends was, in general, slightly higher than that of virgin PLA-V and both reprocessed PLA-R1/R2, offering values in the same order of magnitude. The mechanical blending effectiveness (MBE) increased with the content of reprocessed PLA in the blend, regardless of the type of recycled PLA, so blending could also be considered positive from the mechanical point of view. These results indicated the suitability of PLA-V/R blends to be used in applications with similar mechanical stresses to those of virgin PLA.

The energetic demand for the thermo-oxidative decomposition of PLA-V/R blends was lower and varied in a narrower margin than virgin PLA-V or both reprocessed PLA-R1/R2. Therefore, the energetic valorization of PLA-V/R blends would result in a more feasible process.

To sum up, since the combination of virgin and reprocessed polylactide showed similar processability, service performance and valorization routes to those of virgin polylactide, they could be relevant in the sustainable circular industry of bioplastics.

ACKNOWLEDGMENTS

The authors would like to thank the support of the European Regional Development Fund and the Spanish Ministry of Economy and Competitiveness, through the Research Projects ENE2014-53734-C2-1-R and UPOV13-3E-1947. The Spanish Ministry of Education, Culture and Sports is also thanked for the FPU grant for O. Gil-Castell (FPU13/01916). Generalitat Valenciana is recognized for the APOSTD14/041 program for J.D. Badia. M. Sc. A. Salvador-Andreu is appreciated for his dedication and attitude towards learning. Dr. Llúcia Monreal is acknowledged for her valuable advice. AIMPLAS and GiPC-Eco research group at the UPV are acknowledged for lending processing facilities.

References

1. Y. Ikada and H. Tsuji, Biodegradable polyesters for medical and ecological applications. *Macromol. Rapid Commun.* **21**(3), 117–132 (2000).
2. Y. Doi and A. Steinbuchel (Eds.), *Biopolymers. Polyesters III. Applications and Commercial Products*, vol. 4, Wiley-Blackwell, Weinheim, Germany (2002).
3. A.P. Gupta and V. Kumar, New emerging trends in synthetic biodegradable polymers – Polylactide: A critique. *Eur. Polym. J.* **43**(10), 4053–4074 (2007).
4. A.K. Mohanty, M. Misra, and L.T. Drzal, Sustainable biocomposites from renewable resources: Opportunities and challenges in the green materials world. *J. Polym. Environ.* **10**(1–2), 19–26 (2002).
5. K. Van de Velde and P. Kiekens, Biopolymers: Overview of several properties and consequences on their applications. *Polym. Test.* **21**(4), 433–442 (2002).
6. P. Mapleston, Environmentaly degrading: Bioplastics in Europe. *Plastics Engineering Europe* **Spring**, 24–29 (2006).
7. P. Mapleston, Following the green line: Bioplastics in Europe. *Plastics Engineering Europe* **Winter**, 14–19 (2005).
8. J.-C. Bogaert and P. Coszach, Poly(lactic acids): A potential solution to plastic waste dilemma. *Macromol. Symp.* **153**(1), 287–303 (2000).
9. J.R. Dorgan, H. Lehermeier, and M. Mang, Thermal and rheological properties of commercial-grade poly(lactic acid)s. *J. Polym. Environ.* **8**(1), 1–9 (2000).
10. F. Carrasco, P. Pagès, J. Gámez-Pérez, O.O. Santana, and M.L. Maspoch, Processing of poly(lactic acid): Characterization of chemical structure, thermal stability and mechanical properties. *Polym. Degrad. Stab.* **95**(2), 116–125 (2010).
11. G. Scott (Ed.), *Biodegradable Polymers: Principles and Applications*, 2nd ed., Kluwer Academic Publishers (2002).
12. M. Vert, G. Schwarch, and J. Coudane, Present and future of PLA polymers. *J. Macromol. Sci. Part A. Pure Appl. Chem.* **32**(4), 787–796 (1995).
13. V. Nagarajan, A.K. Mohanty, and M. Misra, Perspective on polylactic acid (PLA) based sustainable materials for durable applications: Focus on toughness and heat resistance. *ACS Sustain. Chem. Eng.* **4**(6), 2899–2916 (2016).
14. K. Meinander, M. Niemi, J.S. Hakola, J. Selin, N.O. Chemicals, T. Centre, and P.O. Box, Polylactides: Degradable polymers or fibres and films. *Macromol. Symp.* **123**, 147–153 (1997).
15. L. Santonja-Blasco, A. Ribes-Greus, and R. G. Alamo, Comparative thermal, biological and photodegradation kinetics of polylactide and effect on crystallization rates. *Polym. Degrad. Stab.* **98**(3), 771–784 (2013).
16. J.R. Rocca-Smith, O. Whyte, C.-H. Brachais, D. Champion, F. Piasente, E. Marcuzzo, A. Sensidoni, F. Debeaufort, and T. Karbowiak, Beyond biodegradability of poly(lactic acid): Physical and chemical stability in humid environments. *ACS Sustain. Chem. Eng.* **5**(3), 2751–2762 (2017).
17. A. Soroudi and I. Jakubowicz, Recycling of bioplastics, their blends and biocomposites: A review. *Eur. Polym. J.* **49**(10), 2839–2858 (2013).
18. F. Vilaplana and S. Karlsson, Quality concepts for the improved use of recycled polymeric materials: A review. *Macromol. Mater. Eng.* **293**(4), 274–297 (2008).

19. R.A.D. Arancon, C.S.K. Lin, K.M. Chan, T.H. Kwan, and R. Luque, Advances on waste valorization: New horizons for a more sustainable society. *Energy Sci. Eng.* **1**, 53–71 (2013).
20. S.M. Al-Salem, P. Lettieri, and J. Baeyens, Recycling and recovery routes of plastic solid waste (PSW): A review. *Waste Manag.* **29**(10), 2625–2643 (2009).
21. I. Pillin, N. Montrelay, A. Bourmaud, and Y. Grohens, Effect of thermo-mechanical cycles on the physico-chemical properties of poly(lactic acid). *Polym. Degrad. Stab.* **93**(2), 321–328 (2008).
22. M. Żenkiewicz, J. Richert, P. Rytlewski, K. Moraczewski, M. Stepczyńska, and T. Karasiewicz, Characterisation of multi-extruded poly(lactic acid). *Polym. Test.* **28**(4), 412–418 (2009).
23. L. Nascimento, J. Gamez-Perez, O.O. Santana, J.I. Velasco, M.L. Maspoch, and E. Franco-Urquiza, Effect of the recycling and annealing on the mechanical and fracture properties of poly(lactic acid). *J. Polym. Environ.* **18**(4), 654–660 (2010).
24. R. Scaffaro, M. Morreale, F. Mirabella, and F.P. La Mantia, Preparation and recycling of plasticized PLA. *Macromol. Mater. Eng.* **296**(2), 141–150 (2011).
25. J.D. Badia, E. Strömberg, S. Karlsson, and A. Ribes-Greus, Material valorisation of amorphous polylactide. Influence of thermo-mechanical degradation on the morphology, segmental dynamics, thermal and mechanical performance. *Polym. Degrad. Stab.* **97**(4), 670–678 (2012).
26. J.D. Badía, E. Strömberg, A. Ribes-Greus, and S. Karlsson, Assessing the MALDI-TOF MS sample preparation procedure to analyze the influence of thermo-oxidative ageing and thermo-mechanical degradation on poly(lactide). *Eur. Polym. J.* **47**(7), 1416–1428 (2011).
27. J.D. Badia and A. Ribes-Greus, Mechanical recycling of polylactide, upgrading trends and combination of valorization techniques. *Eur. Polym. J.* **84**, 22–39 (2016).
28. J.D. Badia, L. Santonja-Blasco, A. Martínez-Felipe, and A. Ribes-Greus, Hygrothermal ageing of reprocessed polylactide. *Polym. Degrad. Stab.* **97**(10), 1881–1890 (2012).
29. J.D. Badia, L. Monreal, V. Sáenz de Juano-Arbona, and A. Ribes-Greus, Dielectric spectroscopy of recycled polylactide. *Polym. Degrad. Stab.* **107**, 21–27 (2014).
30. J.D. Badia, L. Santonja-Blasco, A. Martínez-Felipe, and A. Ribes-Greus, A methodology to assess the energetic valorization of bio-based polymers from the packaging industry: Pyrolysis of reprocessed polylactide. *Bioresour. Technol.* **111**, 468–475 (2012).
31. J.D. Badia, L. Santonja-Blasco, A. Martínez-Felipe, and A. Ribes-Greus, Reprocessed polylactide: Studies of thermo-oxidative decomposition. *Bioresour. Technol.* **114**, 622-628 (2012).
32. F.R. Beltrán, V. Lorenzo, M.U. de la Orden, and J. Martínez-Urreaga, Effect of different mechanical recycling processes on the hydrolytic degradation of poly(l-lactic acid). *Polym. Degrad. Stab.* **133**, 339–348 (2016).
33. E. Strömberg and S. Karlsson, The design of a test protocol to model the degradation of polyolefins during recycling and service life. *J. Appl. Polym. Sci.* **112**(3), 1835–1844 (2009).
34. J.D. Badia, O. Gil-Castell, and A. Ribes-Greus, Long-term properties and end-of-life of polymers from renewable resources. *Polym. Degrad. Stab.* **137**, 35–57 (2017).
35. B. Zhang, X. Bian, S. Xiang, G. Li, and X. Chen, Synthesis of PLLA-based block copolymers for improving melt strength and toughness of PLLA by in situ reactive blending. *Polym. Degrad. Stab.* **136**, 58–70 (2017).
36. K.-W. Lin, C.-H. Lan, and Y.-M. Sun, Poly[(R)3-hydroxybutyrate] (PHB)/poly(l-lactic acid) (PLLA) blends with poly(PHB/PLLA urethane) as a compatibilizer. *Polym. Degrad. Stab.* **134**, 30–40 (2016).
37. H. Liu and J. Zhang, Research progress in toughening modification of poly(lactic acid). *J. Polym. Sci. Part B Polym. Phys.* **49**(15), 1051–1083 (2011).
38. B. Brüster, F. Addiego, F. Hassouna, D. Ruch, J.-M. Raquez, and P. Dubois, Thermo-mechanical degradation of plasticized poly(lactide) after multiple reprocessing to simulate recycling: Multi-scale analysis and underlying mechanisms. *Polym. Degrad. Stab.* **131**, 132–144 (2016).
39. A. Bourmaud, D. Åkesson, J. Beaugrand, A. Le Duigou, M. Skrifvars, and C. Baley, Recycling of L-Poly-(lactide)-Poly-(butylene-succinate)-flax biocomposite. *Polym. Degrad. Stab.* **128**, 77–88 (2016).
40. ISO 291, Plastics. Standard atmospheres for conditioning and testing (1997).
41. J.D. Badia, A. Martinez-Felipe, L. Santonja-Blasco, and A. Ribes-Greus, Thermal and thermo-oxidative stability of reprocessed poly(ethylene terephthalate). *J. Anal. Appl. Pyrolysis* **99**, 191–202 (2013).
42. J.D. Badía, L. Santonja-Blasco, R. Moriana, and A. Ribes-Greus, Thermal analysis applied to the characterization of degradation in soil of polylactide: II. On the thermal stability and thermal decomposition kinetics. *Polym. Degrad. Stab.* **95**(11), 2192–2199, 2010.
43. J.D. Badía, F. Vilaplana, S. Karlsson, and A. Ribes-Greus, Thermal analysis as a quality tool for assessing the influence of thermo-mechanical degradation on recycled poly(ethylene terephthalate). *Polym. Test.* **28**(2), 169–175 (2009).
44. J.D.D. Badia, E. Strömberg, S. Karlsson, and A. Ribes-Greus, The role of crystalline, mobile amorphous and rigid amorphous fractions in the performance of recycled poly (ethylene terephthalate) (PET). *Polym. Degrad. Stab.* **97**(1), 98–107 (2012).
45. O. Gil-Castell, J.D.D. Badia, E. Strömberg, S. Karlsson, and A. Ribes-Greus, Effect of the dissolution time into an acid hydrolytic solvent to tailor electrospun nanofibrous polycaprolactone scaffolds. *Eur. Polym. J.* **87**, 174–187 (2017).
46. O. Gil-Castell, J.D. Badia, T. Kittikorn, E. Strömberg, A. Martínez-Felipe, M. Ek, S. Karlsson, and A. Ribes-Greus, Hydrothermal ageing of polylactide/sisal biocomposites. Studies of water absorption behaviour and physico-chemical performance. *Polym. Degrad. Stab.* **108**, 212–222 (2014).
47. O. Gil-Castell, J.D. Badia, R. Teruel-Juanes, I. Rodriguez, F. Meseguer, and A. Ribes-Greus, Novel silicon microparticles to improve sunlight stability of raw polypropylene. *Eur. Polym. J.* **70**, 247-261 (2015).

48. E.W. Fischer, H.J. Sterzel, and G. Wegner, Investigation of the structure of solution grown crystals of lactide copolymers by means of chemical reactions. *Kolloid Z. Z. Polym.* **251**(11), 980–990 (1973).
49. Y. Song, K. Tashiro, D. Xu, J. Liu, and Y. Bin, Crystallization behavior of poly(lactic acid)/microfibrillated cellulose composite. *Polymer* **54**(13), 3417–3425 (2013).
50. F.A. Dos Santos and M.I.B. Tavares, Development and characterization of hybrid materials based on biodegradable PLA matrix, microcrystalline cellulose and organophilic silica. *Polimeros* **24**(5), 561–566 (2014).
51. V.S. Giita Silverajah, N.A. Ibrahim, W. Md Zin Wan Yunus, H.A. Hassan, and C.B. Woei, A comparative study on the mechanical, thermal and morphological characterization of poly(lactic acid)/epoxidized palm oil blend. *Int. J. Mol. Sci.* **13**(5), 5878–5898, 2012.
52. B.W. Chieng, N.A. Ibrahim, W.M.Z.W. Yunus, M.Z. Hussein, Y.Y. Then, and Y.Y. Loo, Effects of graphene nanoplatelets and reduced graphene oxide on poly(lactic acid) and plasticized poly(lactic acid): A comparative study. *Polymers (Basel)* **6**(8), 2232–2246 (2014).
53. J.D. Badia, L. Santonja-Blasco, A. Martínez-Felipe, and A. Ribes-Greus, Dynamic mechanical thermal analysis of polymer blends, in *Characterization of Polymer Blends: Miscibility, Morphology and Interfaces*, S. Thomas, Y. Grohens, and P. Jyotishkumar (Eds.), pp. 365–392, Wiley-VCH, Weinheim, Germany (2015).
54. B. Baghaei, M. Skrifvars, and L. Berglin, Manufacture and characterisation of thermoplastic composites made from PLA/hemp co-wrapped hybrid yarn prepregs. *Compos. Part A Appl. Sci. Manuf.* **50**, 93–101 (2013).
55. L. Santonja-Blasco, R. Moriana, J.D. Badía, and A. Ribes-Greus, Thermal analysis applied to the characterization of degradation in soil of polylactide: I. Calorimetric and viscoelastic analyses. *Polym. Degrad. Stab.* **95**(11), 2185–2191 (2010).
56. L.A. Pothan, Z. Oommen, and S. Thomas, Dynamic mechanical analysis of banana fiber reinforced polyester composites. *Compos. Sci. Technol.* **63**(2), 283–293 (2003).
57. J.K. Tan, T. Kitano, and T. Hatakeyama, Crystallization of carbon fibre reinforced polypropylene. *J. Mater. Sci.* **25**(7), 3380–3384 (1990).
58. O. Gil-Castell, J.D. Badia, T. Kittikorn, E. Strömberg, M. Ek, S. Karlsson, A. Ribes-Greus, E. Strömberg, M. Ek, S. Karlsson, and A. Ribes-Greus, Impact of hydrothermal ageing on the thermal stability, morphology and viscoelastic performance of PLA/sisal biocomposites. *Polym. Degrad. Stab.* **132**, 87–96 (2016).
59. J.H. Flynn, and L.A. Wall, A quick, direct method for the determination of activation energy from thermogravimetric data, *J. Polym. Sci. Part C Polym. Lett.* **4**(5), 323–328 (1966).
60. T. Ozawa, Kinetic analysis of derivative curves in thermal analysis. *J. Therm. Anal.* **2**(3), 301–324 (1970).
61. H.E. Kissinger, Reaction kinetics in differential thermal analysis. *Anal. Chem.* **29**(11), 1702–1706 (1957).
62. T. Akahira and T. Sunose, Transactions joint convention of four electrical institutes. *J. Sci. Educ. Technol*. **16**, 22–31 (1971).
63. C.D. Doyle, Series approximations to the equation of thermogravimetric data. *Nature* **207**, 290–291 (1965).